L-subshell fluorescence yields for metallic uranium and thorium

J. Q. Xu*
Chinese Center of Advanced Science and Technology (World Laboratory), P.O. Box 8730, Beijing 100080, China

X. J. Xu
Shanghai Institute of Nuclear Research, Academia Sinica, P.O. Box 800-204, Shanghai 201800, China
(Received 6 June 1994; revised manuscript received 31 October 1994)

The L x-ray spectra induced by $\sim$50-keV electron impact on metallic targets of uranium and thorium have been analyzed and the relative fluorescence yields of the L_1, L_2, and L_3 subshell of the two elements, ω_2/ω_3 and ω_1/ω_3, have been derived. The present values of ω_2/ω_3 and ω_2 are notably different from the latest theoretical calculations and semiempirically compiled data, and also from the previous measurements using radionuclide decays to produce initial inner vacancies in the atoms. However, they are reasonable for the theoretical computation of U L x-ray relative intensities induced by a few-MeV proton bombardment on metallic uranium. The deviation is discussed and attributed mainly to an enhancement of the total relaxation effect and the shakeup process in metals with respect to those in the corresponding atomic systems as well as in the chemical compounds.

I. INTRODUCTION

Studies of atomic L-vacancy radiative and radiationless transitions are in rapid progress, and a number of reliable experimental values of the decay parameters, including the L-subshell level widths, $\Gamma(L_i)$, fluorescence yields (ω_i), Auger yields (a_i), Coster-Kronig yields (f_{ij}), etc. ($i=1,2,3$ and $j>i$), are constantly emerging. The latest *ab initio* relativistic theoretical calculations performed in 1981 by Chen, Crasemann, and Mark[1] in the Dirac-Hartree-Slater (DHS) approach generally agree with measurements of the L_2- and L_3-subshell level widths and fluorescence yields, but fail to predict the L_1 subshell yields. Calculations based on the independent-particle model and the frozen-orbital approximation overestimate the L_1-level widths and Coster-Kronig rates by a factor as large as about 2.5 or more, as well as the L_2 Coster-Kronig rates more or less in some elemental regions due to the neglect of many-body and solid effects. Since that time, some improved treatments related to relativity, exchange, electron correlation, relaxation, and solid effects have been put forward.[2–6] However, the need for more experimental information to guide the theoretical work is pronounced.

On the experimental side, the selective photoionization of consecutive L subshells by monochromatized synchrotron radiation produces the desired single-initial-vacancy state, and by means of this technique a large quantity of data on the L-subshell yields have been obtained.[7–10] The improved method using radionuclide sources and coincidence techniques for measuring the yields ω_2, ω_3, and f_{23} of heavy elements has reduced its experimental uncertainties in recent years.[11–13] Careful measurements with a high-resolution crystal spectrometer provided many L subshell level widths[14,15] and fluorescence yields.[16] Analyses of the diagram and satellite L x-ray spectra induced by photon, electron, and proton impact have brought about fuller information concerning the M-electron shakeup and shakeoff events, the L_1-L_2M and L_1-L_3M Coster-Kronig transitions, and the L-subshell fluorescence yields.[17–19] However, it has been found that some of those experimental values reported in the last decade are not only different from the latest theoretical calculations, the semiempirical compilations by Krause and Oliver,[20] and many old measurements, but also from each other; examples are the unexpected deviation between the values measured by using the method of the synchrotron-radiation ionization of elemental metals and by using the radionuclide source and coincidence technique for the L_2-L_3 and L_1-L_2 Coster-Kronig yields of elements with atomic number $Z\approx 80$ (Refs. 7 and 12), and for the Sm L_1-L_3 Coster-Kronig yield.[9]

In this work, we will study the L-subshell fluorescence yields of uranium and thorium in the metallic state. Previous studies of U and Th L-vacancy transition yields have proven to be replete with various difficulties: effective measurements are scarce, the reported data are scattered, and not much information about their neighboring elements can be obtained. In the past decade, to our knowledge, only one measurement of U $L_{2,3}$ subshells was published, which was carried out using a radioactive ^{235}Np source by McGhee and Campbell.[12] Their measured values of ω_2 and ω_3 for uranium disagree with the latest calculation and the compilation, although the experiment was carefully checked and reproduced. The ratio of ω_2/ω_3 to be derived in this work from the L x-ray spectrum produced by electron impact on metallic uranium also deviates from the latest calculation and the semiempirical compilation, and even from the measurement of McGhee and Campbell. In the present work, we will give a qualitative explanation of the variation by resorting to solid-state effects. Some experiments have indicated that, for a given element, accompanying the condensation of free atoms to elemental metal, the atomic

electron binding energies will decrease by several eV, and the Auger transition energies and rates will be changed.[21,22] In general, the Coster-Kronig decay processes are rather sensitive to binding and decay energies.

Additionally, in the field of atomic inner-shell ionization and L x-ray spectroscopy, the lack of correct knowledge of the L-subshell vacancy decay yields makes it difficult to derive the L-subshell ionization cross sections from directly measured x-ray intensities. The pronounced discrepancy between the ion-induced relative L-subshell ionization cross sections (or relative x-ray intensities) predicted by theoretical calculations and measured experimentally has stood for 20 years,[23] and was found to be serious for heavy elements, especially for uranium.[24] In those calculations Krause's compiled values of the decay yields of heavy elements were used, which were evaluated in 1979 mainly on the basis of some theoretical calculations and experimental data measured by employing radionuclides in chemical compounds. To interpret and remove the L-subshell-related discrepancy between theory and measurements, in recent work[25] we adopted the fluorescence yields of elemental metals in calculations of Au, Pb, and Bi L x-ray intensities, and found that the calculated results are in good agreement with measurements for few-MeV proton and ^{4}He-ion bombardment on metallic targets. Therefore, it is significant for clearing the air to obtain more experimental values of the L-subshell yields by employing various techniques and specimens.

II. L-SUBSHELL FLUORESCENCE YIELDS

In the present study, the L x-ray spectra of U and Th reported by Goldberg[26] are used to derive the relative fluorescence yields. He measured the relative L-line intensities induced by electrons in an x-ray tube worked at a voltage $\sim$50 kV and a current $\sim$25 mA and recorded with a curved mica crystal bent to a cylinder of 40-cm radius. The uranium metal and thorium alloy (30 at.% Th+70 at.% Cu) were covered, respectively, with copper and then soldered on a copper supporter on the tube anode. His results related to this work are listed in Table I, but some of them are recalculated in light of the corrected data given in Ref. 27. The listed errors of the x-ray intensities, I_1, I_2, and I_3, are estimated from the experimental errors of individual lines reported in Ref. 27.

TABLE I. Relative intensities of the L_1-, L_2-, and L_3-subshell x-ray lines measured by Goldberg (Ref. 26), ionization cross-section ratios for 50-keV electron impact on U and Th (Ref. 28), and present fluorescence yields.

	U	Th	Error
I_1	11.0	11.4	7%
I_2	52.8	55.6	8%
I_3	144	146	2%
σ_3/σ_1	3.847	3.718	4%
σ_2/σ_1	1.180	1.183	4%
ω_3	0.398[a]	0.386[b]	3%
ω_2	0.553	0.532	9%
ω_1	0.142	0.136	9%

[a]From the measurement by McGhee and Campbell (Ref. 12).
[b]Assumed (see text).

The L-subshell fluorescence yields are related to the L_i-subshell ionization cross sections σ_i, x-ray emission intensities I_i, and Coster-Kronig yields f_{ij}, as follows:[19]

$$\omega_1/\omega_3=(\sigma_3/\sigma_1+f_{23}\sigma_2/\sigma_1+f_{13}+f_{12}f_{23})(I_1/I_3)\ , \tag{1}$$

$$\omega_2/\omega_3=(\sigma_3/\sigma_1+f_{23}\sigma_2/\sigma_1+f_{13}+f_{12}f_{23})\times(I_2/I_3)/(\sigma_2/\sigma_1+f_{12})\ . \tag{2}$$

In this computation, the ratios of ionization cross sections for 50-keV electrons are from Scofield's work,[28] which were calculated relativistically in the first-order Born approximation and are listed in Table I (interpolated for Th). The ionization cross sections of Scofield have been tested by a recent measurement of Reusch *et al.*,[29] using a flat crystal spectrometer to measure the L x rays induced by electrons with energies $50\le E\le 200$ keV, and the comparison between them displays a good agreement for heavy elements. The Coster-Kronig yields are from the latest theoretical calculations of Chen, Crasemann, and Mark,[1] which seem more reasonable than the compiled data of Krause[20] for the heavy elements.[7,12] The ratio forms of the L_i-subshell x-ray intensities and ionization cross sections are beneficial to a reduction of systematic errors of the calculated results. The computed results are

$$\omega_1/\omega_3(\mathrm{U})=0.357\ , \tag{3}$$

$$\omega_2/\omega_3(\mathrm{U})=1.39\ , \tag{4}$$

$$\omega_1/\omega_3(\mathrm{Th})=0.352\ , \tag{5}$$

$$\omega_2/\omega_3(\mathrm{Th})=1.38\ . \tag{6}$$

The latest experimental value for the U L_3-subshell fluorescence yield, $\omega_3(\mathrm{U})=0.398\pm0.006$, was reported in 1988, and measured by McGhee and Campbell[12] by using a ^{235}Np radioactive source and a K x-ray–L x-ray coincidence technique. This value is plotted in Fig. 1, and is in line with the experimental data reported in recent years for other heavy elements.[12,19,25,30–32] The figure shows that almost all these data are less than the theoretical and semiempirical values. In the same year, Amorim *et al.*[15] measured with a curved quartz crystal the widths $\Gamma(La_1)$ and $\Gamma(La_2)$ of the La_1 and La_2 lines induced by $\sim$35-keV electron bombardment on metallic gold, thorium, and uranium. Prior to that measurement, Laakkonen and co-workers[33] published the widths of the Ma_1 and $M\beta$ lines of the three elemental metals, produced by a Cr (or Mo) x-ray fluorescence tube and recorded with a double-quartz-crystal spectrometer; and Fuggle and Alvarado[34] reported the N_6- and N_7-subshell widths determined by x-ray photoelectron spectroscopy. Those data are given in Table II. From them and the expressions

$$\Gamma(L_3)=\Gamma(L\alpha_1)-[\Gamma(M\alpha_1)-\Gamma(N_7)]\ , \tag{7}$$

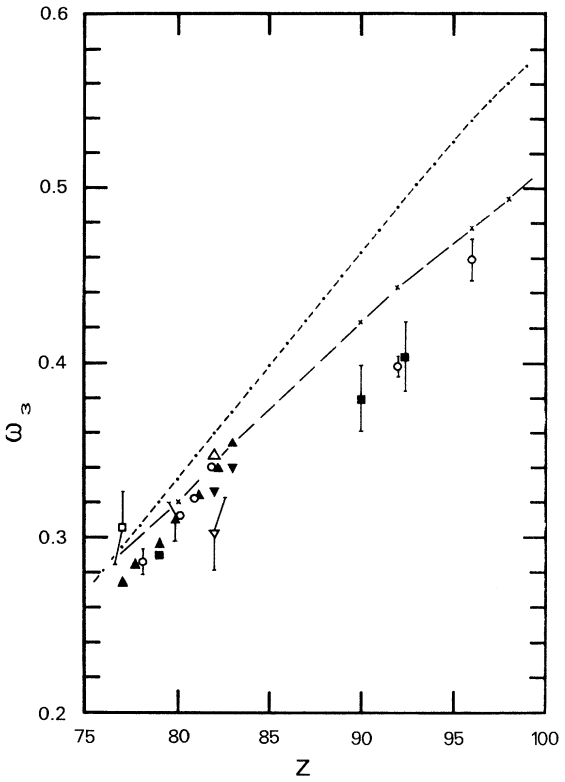

FIG. 1. L_3-subshell fluorescence yield ω_3 as a function of atomic number Z. Small dots and crosses are the compiled (Ref. 20) and the latest theoretical data (Ref. 1) and connected by lines to guide the eye. Experimental data: ○, McGhee and Campbell (Ref. 12); △, Kodre *et al.* (Ref. 30); ▽, Tan, Braga, and Fink (Ref. 31); □, Rao (Ref. 32); ▲, Xu (Ref. 19); ▼, Xu (Ref. 25); ■, Amorim *et al.* (Ref. 15) (see text). Some representative error bars are plotted.

TABLE II. Experimental $L\alpha_{1,2}$-, $M\alpha_1$-, and $M\beta$ linewidths and N_6- and N_7-level widths (in eV) for metallic gold, thorium, and uranium.

Element		Amorim *et al.* (Ref. 15)	Laakkonen and co-workers (Ref. 33)	Fuggle and Alvarado (Ref. 34)
Au	$L\alpha_1$	7.78±0.12		
	$L\alpha_2$	8.08±0.16		
	$M\alpha_1$		2.32±0.2	
	$M\beta$		2.32±0.2	
	$N_{6,7}$			0.41
Th	$L\alpha_1$	11.82±0.58		
	$L\alpha_2$	11.80±0.42		
	$M\alpha_1$		3.8±0.2	
	$M\beta$		4.1±0.2	
	$N_{6,7}$			0.75±0.16
U	$L\alpha_1$	12.02±0.57		
	$L\alpha_2$	12.11±0.61		
	$M\alpha_1$		3.8±0.2	
	$M\beta$		3.9±0.2	
	$N_{6,7}$			0.76±0.17

$$\Gamma(L_3)=\Gamma(L\alpha_2)-[\Gamma(M\beta)-\Gamma(N_6)]\ , \tag{8}$$

we have $\Gamma(L_3)=6.02$ eV for Au, 8.61 eV for Th, and 8.98 eV for U. By means of the basic relation $\omega_3=\Gamma_R/\Gamma(L_3)$, and the Dirac-Fock (DF) values of the L_3-subshell x-ray emission rates[35,36] Γ_R, the L_3-subshell fluorescence yields ω_3(Au)=0.290, ω_3(Th)=0.380, and ω_3(U)=0.403 are obtained, which are also plotted in Fig. 1. The three data are well in accord with the other experimental ones. By adopting the value of ω_3(U)=0.398 of McGhee and Campbell and assuming ω_3 (Th)=0.386 (see Fig. 1), the yields of ω_1 and ω_2 are calculated from Eqs. (3)–(6), and the results are given in Table I.

McGhee and Campbell[12] also presented the U L_2-subshell fluorescence yield ω_2(U)=0.457±0.014, but it was calculated from the other values derived experimentally. The L_2-subshell Coster-Kronig transition rates and then the fluorescence yield may be sensitive to multiple-hole states and solid effects. Hence the ω_2(U) value is not adopted in the present work.

III. DISCUSSION

The recent experimental ω_2 values for heavy elements,[7,12,19,25,30–32] together with the latest theoretical calculations of Chen, Crasemann, and Mark[1] and the semiempirically compiled data of Krause,[20] are given in Fig. 2. The figure shows that, for U and Th, the present

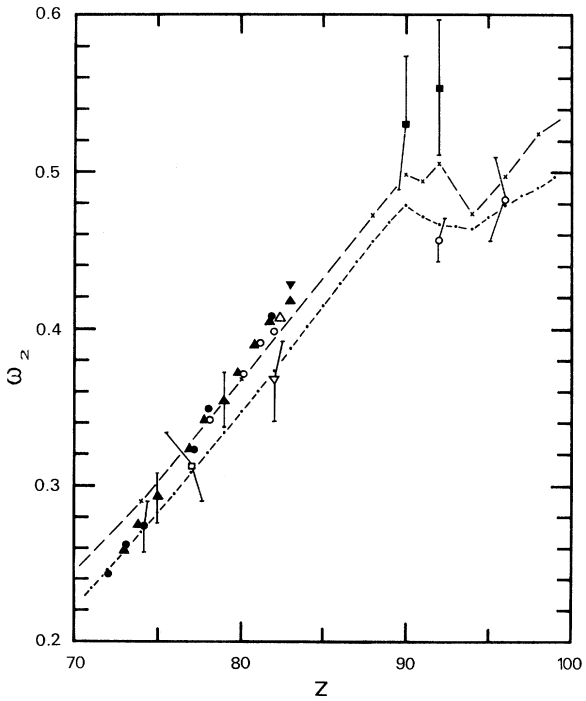

FIG. 2. L_2-subshell fluorescence yield ω_2 as a function of atomic number Z. Small dots and crosses are the compiled (Ref. 20) and latest theoretical data (Ref. 1), and are connected by lines to guide the eye. Experimental data: ●, Werner and Jitschin (Ref. 7); ■, present values; for definition of the other symbols, see the caption to Fig. 1.

TABLE III. Relative L_2- and L_3-subshell fluorescence yields ω_2/ω_3 for elements U and Th.

	U	Th	
Krause (Ref. 20)	0.955	1.03	Semiempirical
Chen, Crasemann, and Mark (Ref. 1)	1.14	1.18	Theoretical
McGeorge *et al.* (Ref. 37)	1.16±0.10		Radionuclide
McGhee and Campbell (Ref. 12)	1.15±0.04		Radionuclide
Present	1.39±0.12	1.38±0.12	Metallic

ω_2 values are remarkably greater than the measurement by McGhee and Campbell. Krause argued when compiling the L_2-subshell yields of the elements with atomic numbers from $Z=88$ to 96 that ω_2 values could not lie above his compiled data for a given Z, otherwise these values would not be accommodated within the systematics of the tendency of the radiative and Auger rates adopted in his compilation. However, we know from Fig. 2 that the present two values are in accord with the tendency toward a more rapid increase of the recent experimental yields with increasing the atomic number in the range $72 \leq Z \leq 83$. Krause's systematics for heavy elements is questionable.

The ratios of ω_2/ω_3 for the investigated elements are listed in Table III. Both the measurements of McGhee and Campbell[12] and McGeorge *et al.*[37] for uranium, carried out with a radionuclide ^{235}Np source and a K-L x-ray coincidence technique, are in excellent agreement with the theoretical calculations, but they are different from the compiled and present values. More experimental data on ω_2/ω_3 for heavy elements are given in Fig. 3. The results of Werner and Jitschin[7] were obtained by making use of the synchrotron photoionization of the metallic targets. The data of Xu[25] were from the L x-ray spectra produced by electron and proton impact on the elemental metals. The two ω_2/ω_3 values for Cm, presented by McGhee and Campbell[12] and McGeorge and Fink,[38] respectively, were measured by using a ^{249}Cf source and a K-L x-ray coincidence technique, and agree well with each other (note that different ω_2 and ω_3 values at $Z=92$ and 96 were obtained by the two research groups, which may be due to some unknown systematic problems). Figure 3 shows that the ω_2/ω_3 measurements obtained by using the radionuclide and coincidence techniques better follow the theoretical prediction, that the values for photon, electron, and proton impacts on metallic targets appear to be well in line, and that the compiled values are the smallest by comparison. In the following text, we will first test the present values for uranium and then explain the deviations by virtue of the metallic effects.

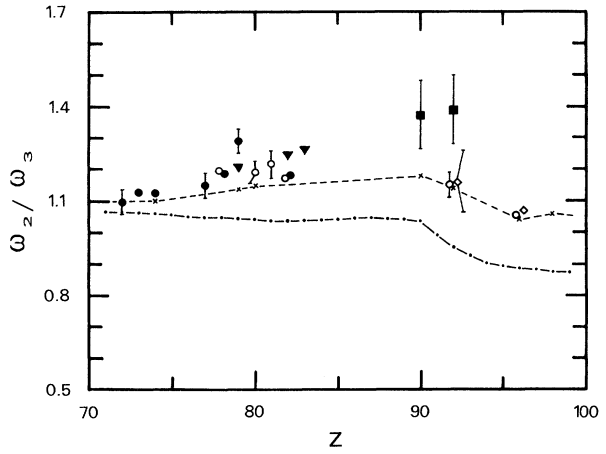

FIG. 3. Relative fluorescence yield of the L_2 and L_3 subshells as a function of atomic number Z. Experimental data: ○, McGhee and Campbell (Ref. 12); ◇, McGeorge and co-workers (Refs. 37 and 38); ●, Werner and Jitschin (Ref. 7); ▼, Xu (Ref. 25); ■, present values. The open symbols denote the measurements using a radionuclide in a chemical compound, whereas the solid ones refer to the experiments in which a metallic target was used. For a definition of the two curves, see the caption to Fig. 1.

A. Test of the values of U L-subshell fluorescence yields

To test primarily the present L-subshell fluorescence yields, we computed the relative intensities between the $L\beta$, $L\gamma$, L_{total}, and $L\alpha$ x-ray lines, i.e., I_β/I_α, I_γ/I_α, and I_T/I_α, for a few-MeV proton impact on metallic uranium foils. The L x-ray production cross sections $\sigma_\rho(L_i)$ for the L_ρ-line transition to the L_i subshell ($i=1$, 2, and 3) are given by

$$\sigma_\rho(L_1)=\sigma_1\omega_1\Gamma_\rho/\Gamma_R(L_1)\ , \tag{9}$$

$$\sigma_\rho(L_2)=(\sigma_2+\sigma_1 f_{12})\omega_2\Gamma_\rho/\Gamma_R(L_2)\ , \tag{10}$$

$$\sigma_\rho(L_3)=[\sigma_3+\sigma_2 f_{23}+\sigma_1(f_{13}+f_{12}f_{23})]\omega_3\Gamma_\rho/\Gamma_R(L_3)\ . \tag{11}$$

The L x-ray relative intensities for thin targets are given by the ratio of production cross sections,

$$I_\rho/I_\alpha=\sigma_\rho/\sigma_\alpha\ , \tag{12}$$

where ρ denotes β, γ, etc. The L x-ray lines considered in this work are $L\alpha_{1,2}$, $L\beta_1$ to $L\beta_7$, $L\beta_{15}$, and $L\gamma_1$ to $L\gamma_6$, $L\gamma_8$, L_l and L_η. In the above equations, $\Gamma_\rho/\Gamma_R(L_i)$ is the fractional radiative width of the L_ρ-line transition, and the DF values of Γ_ρ and $\Gamma_R(L_i)$ (Ref. 35) tabulated by Campbell and Wang[36] were adopted in the present computations. It has been pointed out[36,39] that the DF L x-ray emission rates are potentially more accurate than the previous Hartree-Slater (HS) values.[40] The Coster-Kronig yields f_{ij} are from the latest theoretical

calculations.[1] Here σ_i is the ion-induced L_i-subshell ionization cross section, and ECPSSR values[41] were employed. ECPSSR is abbreviated from the plane-wave Born approximation with corrections for particle-energy loss (E), Coulomb deflection (C), perturbed stationary state (PSS), and relativistic effects (R),[42] and has been widely used in atomic physics. A recent work of the authors[25] demonstrated clearly that the ECPSSR L-subshell ionization cross sections are justified at least for heavy elements and protons with energies more than 1 MeV. Just recently, the work by Dhal, Nandi, and Padhi[43] also showed that their experimental x-ray production cross-section ratios for 1–2-MeV/amu α particle bombardment on pure Pb and Bi targets are in good agreement with the theoretical calculations obtained by using the ECPSSR cross sections and the fluorescence yields presented by us. As mentioned in many publications, the measured ratios of x-ray intensities (or cross sections) provide a rigorous test of theoretical predictions and the related parameters because many uncertainties of them are canceled or reduced.

The computations of I_β/I_α, I_γ/I_α, and I_T/I_α were performed in the following four cases. In cases A and B, the compiled and theoretical fluorescence yields ω_i were used, respectively. In case C, the experimental ω_2 and ω_3 values of McGhee and Campbell[12] and the theoretical ω_1 were adopted. The result in case D was calculated by using the present ω_i values listed in Table I. The computed results are given in Fig. 4, together with some experimental data collected from the compilation by Sokhi and Crumpton.[44] In comparison with the experimental data, the ECPSSR x-ray intensity ratio calculated in case D (solid lines) is by far the best of the four results. The case A calculation (the slashed-dashed lines) is the worst, and both the case B (chain lines) and case C (broken lines) ones also fail to reproduce the measured data.

For uranium targets and incident protons with energies more than 1 MeV, the ECPSSR cross section σ_3 is more than both the σ_2 and σ_1 for a given proton energy, and the L-subshell Coster-Kronig yields are by definition less than unity: $f_{12}=0.051$, $f_{13}=0.656$, and $f_{23}=0.138$.[1] Hence the intensity ratio I_ρ/I_α depends essentially upon the relative yields of ω_2/ω_3 and ω_1/ω_3, relative cross sections of σ_2/σ_3 and σ_1/σ_3, and relative x-ray emission rates; the ratio forms are beneficial to reduction of the systematic errors of the computed results. Therefore, the origin of the deviations of the four calculations given in Fig. 4 stems mainly from the different values of ω_2/ω_3 adopted in the four cases. Case B and case C calculations accord well with each other because the ω_2/ω_3 values used in the two cases are nearly the same. This test demonstrates that the present value of ω_2/ω_3 is much more reasonable than the others for proton-induced ionization of metallic uranium. Incidentally, by observing the values of the ECPSSR ionization cross sections and the L-subshell Coster-Kronig yields for heavy elements, one will know that when proton energy $E \gtrsim 1$ MeV, the ECPSSR L x-ray relative intensities I_ρ/I_α are strongly dependent on the relative fluorescence yields, whereas when $E \lesssim 0.5$ MeV the relative intensities are not only dependent on the relative fluorescence yields but also obviously on the Coster-Kronig yields.

In addition, another often-used ionization theory for proton impact is the RPWBA-BC,[45] which was developed from the plane-wave Born approximation (PWBA), and the relativistic (R) ionization cross sections were evaluated with Dirac-Hartree-Slater (DHS) wave functions and include binding (B), polarization, and Coulomb deflection (C) corrections. In recent studies,[25,46] the RPWBA-BC and ECPSSR ionization cross sections, together with the theoretical DHS decay yields[1] and recent experimental fluorescence yields, respectively, were applied to calculate some L x-ray relative intensities, such as I_β/I_α, I_γ/I_α, $I_{\gamma 1}/I_\alpha$, etc., for proton impact on heavy elements. The calculations show that the RPWBA-BC x-ray relative intensities agree well with measurements for proton energies $1<E<3$ MeV while the ECPSSR ones cover a greater energy region. Therefore, we adopted the ECPSSR values in this test. The present ECPSSR values of U $L\alpha$, $L\beta$, $L\gamma$, and total L x-ray production cross sections in case D for 1–5-MeV

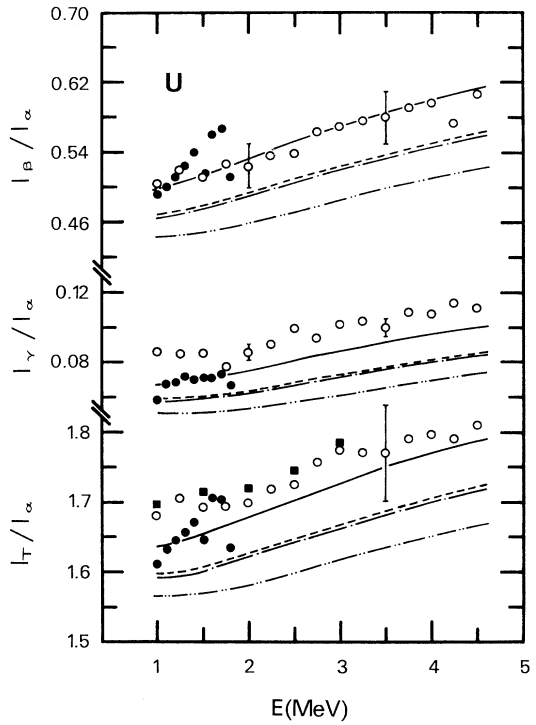

FIG. 4. Intensity ratios of U $L\beta$, $L\gamma$, and total L x-ray to $L\alpha$ line as a function of proton energy E. The experimental data, from Bhattacharya *et al.* (●), Leite *et al.* (■), and Tawara *et al.* (○), are collected from the data tables by Sokhi and Crumpton (Ref. 44). Present calculations: —··—·· computed by using the compiled L-subshell fluorescence yields, ω_i (Ref. 20); —·—·—·, computed by using the theoretical ω_i values (Ref. 1) — — —, computed by using the theoretical ω_1 (Ref. 1) and the experimental ω_2 and ω_3 values of McGhee and Campbell (Ref. 12); ——, computed by using the present ω_i values. In those calculations, the ECPSSR ionization cross sections (Ref. 41) and the Dirac-Fock x-ray emission rates (Ref. 36) are employed.

TABLE IV. Ratios of U $L\alpha$, $L\beta$, $L\gamma$, and total L x-ray production cross sections computed using the ECPSSR (Ref. 41) and the RPWBA-BC ionization cross sections (Ref. 45), together with the present fluorescence yields and the DHS decay yields (Ref. 1), respectively. In these computations the DF emission rates (Ref. 36) were used. Proton energy E ranges from 1 to 5 MeV.

E	$L\alpha$	$L\beta$	$L\gamma$	L_T
1.0	1.07	1.04	0.99	1.06
1.5	1.07	1.05	1.03	1.06
2.0	1.04	1.03	1.01	1.04
2.5	1.02	1.01	0.99	1.01
3.0	1.00	0.99	0.98	1.00
3.5	0.99	0.98	0.98	0.99
4.0	0.98	0.99	0.99	0.98
5.0	0.97	0.99	1.01	0.98

protons are in good agreement with the RPWBA-BC calculations using the DHS decay yields and DF emission rates; a comparison between them is given in Table IV. The recently published compilation of experimental L-shell x-ray production and ionization cross sections for proton impact by Orlic, Sow, and Tang[44] may be useful for further examination of the two ionization theories.

B. Interpretation of the deviations

The present ω_2 values and the ratios of ω_2/ω_3 obtained from reported experiments of electron impact on metallic uranium and thorium are much larger than the theoretical and compiled data and than measurements using the radionuclide and coincidence techniques (see Figs. 2 and 3). The Auger process is less sensitive to the electron binding energy than the Coster-Kronig transition. From the basic relation $\omega_2+a_2+f_{23}=1$, we know that the increase of ω_2 for U and Th metals probably leads to a decrease in the f_{23} values. This situation is accommodated within the systematics of the experimental f_{23} values of the elements with $Z=72-82$, measured by employing the synchrotron photoionization of the pure elemental foils, which are plotted in Fig. 5 together with the theoretical and compiled data. The figure also shows that the onset of the L_2-L_3M Coster-Kronig process is located at $Z=91$, and the L_2-subshell Coster-Kronig processes for $Z\leq 90$ are referred to as the L_2-L_3Y transitions (Y denotes the N, O, P, and Q shells). The square symbol at $Z=90$ in Fig. 5 is an approximation for guiding the eye, which is estimated by using the present $\omega_2=0.532$ and assuming that the Auger yields of the Th L_2-subshell are not changed when the system alters from free atoms to the metallic state. By the same token, the L_2-L_3Y transition yield of metallic uranium will also drop sharply.

In Fig. 5, the measurements using the radionuclide and coincidence techniques of McGhee and Campbell,[12] Catz and Meyers[13] and Semmes *et al.*[47] are in good agreement with the compiled data for $Z<90$, though on an average the former are a little lower. This is not strange because the compiled f_{23} values for these elements were evaluated in 1979 mainly from the existing experimental data measured via vacancy production through nuclear disintegrations. In the range from $Z=70$ to 90, the theoretical calculations are a little higher, but Werner and Jitschin's values are obviously lower than the compiled data. Werner and Jitschin did not present a clear interpretation of the origin of the unexpected deviation; they suggested only that it might stem from unrecognized instrumental problems or from the different ways of initial vacancy creation. Just recently, Stötzel *et al.* of that research group[9] again found that their value for the Sm L_1-L_3Y transition, $f_{13}=0.18\pm0.03$, measured by using the same method, was surprisingly smaller than the existing data, predicted by the latest theoretical calculation ($f_{13}=0.332$), compiled by Krause ($f_{13}=0.30\pm0.03$), and extrapolated from previous experimental values of its neighboring elements. By observing the theoretical energies of Sm L_1-L_3 Coster-Kronig transitions, they deemed that multielectron effects are of minor importance for theoretical calculations, and that any possible coupling between the radiative and radiationless transitions should not significantly affect the transition rates.

It is natural that the different mechanisms for creating

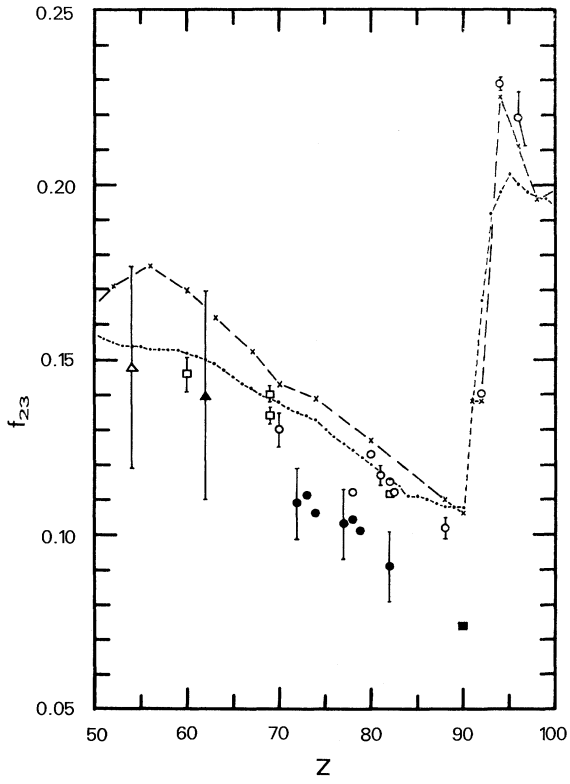

FIG. 5. L_2-L_3 Coster-Kronig transition yield f_{23} as a function of atomic number Z. Experimental data: ○, McGhee and Campbell (Ref. 12); □, Catz and Meyers (Ref. 13); △, Semmes *et al.* (Ref. 47); ●, Werner and Jitschin (Ref. 7); ▲, Stötzel *et al.* (Ref. 9); ■, present estimate (see text). For definition of the two curves, see the caption to Fig. 1. The open symbols denote the measurements using a radionuclide in a chemical compound, whereas the solid ones refer to the experiments in which a metallic target was used.

initial vacancies affect more or less the Coster-Kronig transition yields. However, it is known from Figs. 3 and 5 and the above description that the different types of radionuclides (creating different initial vacancy distributions due to the α, β^-, and electron-capture decays) evidently do not hinder the experimental f_{23} data from their consistency, and that the different types of L-shell ionization by photon, electron, and proton impacts on specimens of metallic foils bring about better-matched f_{23} and ω_2/ω_3 values. This indicates that the effect of the mechanisms of initial vacancy production on the f_{23} yield for heavy elements is slight, and that f_{23} values are potentially classified due to the different specimens used in the experiments. One should bear in mind that the theoretical work is carried out on an atomic system, whereas the experimental subjects are generally solid specimens except for inert gases, and further that the specimens used in the radionuclide and coincidence techniques are always chemical compounds (salts), whereas the targets impacted by photon, electron, and proton beams are often elemental metals (sometimes alloy foils are used). Hence the deviation of the f_{23} values in the two cases (compounds and metals) can probably be ascribed mainly to the physical and chemical environments in which the investigated atom exists.

The Coster-Kronig energies, which depend on the binding energies of the atomic-orbital electrons, greatly affect the transition rates. In an atomic system, the Coster-Kronig electron energy for an L_i-L_jX_k transition process ($i=1$, 2, and 3; $j>i$; X denotes an outer shell), assuming that the electron orbitals from the initial to the final states are frozen and the process is possible, can be expressed in the form

$$\begin{aligned} E_{\rm ck}(L_i-L_jX_k)_{\rm at} &= E[L_i]_{\rm ion}-E[L_jX_k]_{\rm ion} \\ &= \mathcal{E}(L_i)-\mathcal{E}(L_j)-\mathcal{E}(X_k)-\mathcal{J}(L_j,X_k)\ , \end{aligned} \tag{13}$$

where ck indicates that the Coster-Kronig process arises in an atomic system; $E[L_i]_{\rm ion}$ and $E[L_jX_k]_{\rm ion}$ stand for the total energy of an ion with a single hole in the L_i subshell and with two single holes in the L_j and X_k subshells, respectively; $\mathcal{E}(L_i)$, $\mathcal{E}(L_j)$, and $\mathcal{E}(X_k)$, respectively, denote the binding energy of an electron in each of the three subshells; and $\mathcal{J}(L_j,X_k)$ denotes the interaction energy of the two final-state holes in the L_j and X_k orbitals. When the adiabatic relaxation effect is included, which always occurs due to a change of the electronic charge of the atom (or ion), this expression can be rewritten within an intermediate-coupling model as follows:[21,48]

$$\begin{aligned} E_{\rm ck}(L_i-L_jX_k)_{\rm at,R} &= E_{\rm ck}(L_i-L_jX_k)_{\rm at}+\mathcal{R}_{\rm at}(L,X) \\ &= \mathcal{E}(L_i)-\mathcal{E}(L_j)-\mathcal{E}(X_k)-\mathcal{J}(L_j,X_k) \\ &\quad +\mathcal{R}_{\rm at}(L,X)\ . \end{aligned} \tag{14}$$

Here the adiabatic relaxation correction term, $\mathcal{R}_{\rm at}(L,X)$, accounts for the decrease in the final-state energy resulting from the atomic orbital contraction due to the altered electronic structure of the free atom. The value of $\mathcal{R}_{\rm at}(L,X)$ is nearly independent of the involved subshells, but depends upon the principal quantum numbers of shells containing the holes. In a heavy atom only the relaxation of outer shells is of importance.

In metals, there exist many free electrons in the conduction band. As soon as a core hole is created in an atomic shell, the free electron will move from other parts of the conductive metal to try to screen the localized positive ion in the ionization process, and thus the initial state of the Coster-Kronig transition in the metal approximately corresponds to a system with an extra conduction electron in the vicinity of the ion; that is, the screening of the core hole by valence-band electrons is increased with respect to that in the corresponding free-atom system. This process is referred to as extra-atomic relaxation,[49,50] which is strongly dependent on the electronic property of the material. The extra-atomic relaxation energies are determined by more long-range Coulomb interactions, and depend mainly upon the charge of the ion; i.e., this metal-state correction is approximately a characteristic of the element, and is nearly independent of the exact nature of the shells and the radiationless transition process.[49-51] It always tends to lessen the electron binding energies, i.e., for a given element

$$\mathcal{E}_{\rm met}<\mathcal{E}_{\rm at}\ , \tag{15}$$

and thus increases the radiationless transition energies for a system from the vapor to the metallic state. Therefore, the Coster-Kronig energy in a metallic system[21,51,52] is expressed by

$$\begin{aligned} E_{\rm ck}(L_i-L_jX_k)_{\rm met,R} &= E_{\rm ck}(L_i-L_jX_k)_{\rm met}+\mathcal{R}_{\rm at}(L,X)+\mathcal{R}_{\rm ext}(Z) \\ &= \mathcal{E}(L_i)_{\rm met}-\mathcal{E}(L_j)_{\rm met}-\mathcal{E}(X_k)_{\rm met}-\mathcal{J}(L_j,X_k) \\ &\quad +\mathcal{R}_{\rm at}(L,X)+\mathcal{R}_{\rm ext}(Z)\ , \end{aligned} \tag{16}$$

where the met and ext subscripts stand for the metallic system and the extra-atomic relaxation, respectively. The extra-atomic relaxation energy $\mathcal{R}_{\rm ext}(Z)$, which is related to the total metal-state contribution to the Coster-Kronig electron energy, depends on atomic number Z and is about a few eV.[22,51,53] Hence in metals the relaxation energy $\mathcal{R}_{\rm met}$ is the sum of the atomic relaxation energy $\mathcal{R}_{\rm at}$ and the extra-atomic relaxation energy $\mathcal{R}_{\rm ext}$, i.e.,

$$\mathcal{R}_{\rm met}=\mathcal{R}_{\rm at}+\mathcal{R}_{\rm ext}\ . \tag{17}$$

In a chemical compound $\mathcal{R}_{\rm ext}$ is very small because of the lack of such free charges, and so the vacancy transition processes are more similar to those in the corresponding atomic system. It is worthwhile to remember that for a radiative transition both the atomic relaxation and extra-atomic relaxation effects on the x-ray energy and emission rate are slight since there is no change in the charge state of the studied atom.[51,54]

Note that the electron binding energies for atomic systems refer to the vacuum level while those for solid states refer to the Fermi level, since there exists a continuum of levels available above the Fermi level and the outgoing

electrons need not escape from the solid. A common approach to express the solid-state binding energy relative to the vacuum level is given by

$$\mathcal{E}(\text{vacuum})=\mathcal{E}(\text{Fermi})+\varphi(Z)\ , \tag{18}$$

where $\varphi(Z)$ is the work function of the elemental metal with atomic number Z; for example, φ (W)=4.55 eV, φ (Au)=5.1 eV, and φ (U)=3.63 eV.[55] For chemical compounds, particularly insulators, the choice of a reference level is more difficult because of localized charging of the experimental specimen.

Concerning the Coster-Kronig transition rates, the theoretical calculations for atomic systems by Karim, Chen, and Crasemann[2] and Fritzsche, Fricke, and Sepp[5] have shown that the free-atomic relaxation reduces the L_1-subshell rates from a few percent to about 10%; for example, about 12% for Ar L_1-$L_{2,3}M_1$ and 10–20 % for Zn L_1-$L_{2,3}X$ transitions. For L_2-subshells, the reduction of the Coster-Kronig rates will be smaller *a priori* since the L_2-subshell Coster-Kronig electrons have higher energies. Moreover, recent work by Tulkki and Mäntykenttä[54] indicated that the atomic relaxation effect depends not only on the energy of the outgoing electron, but also on the number of electrons in subshells above the final-state holes, and that when the atomic number Z increases the atomic relaxation effect becomes larger resulting in more reduction of the transition rates. In consequence, inclusion of extra-atomic relaxation in a metal will reduce the Coster-Kronig rate further with respect to the relaxation in the corresponding atomic system if the transition is possible, because the total relaxation energy due to a core hole increases from $\mathcal{R}_{\text{at}}$ in free atoms to $\mathcal{R}_{\text{at}}+\mathcal{R}_{\text{ext}}$ in the metallic state.

In addition, we should investigate how the electron shakeup and shakeoff events that precede the Coster-Kronig transitions change when an atomic system alters to the metallic one. These events are an atomic process by which an orbital electron is excited automatically with a given probability either into an unoccupied outer orbital (shakeup) or into the continuum (shakeoff, in an atomic system) as the consequence of a sudden change in the effective charge felt by that orbital electron. This change can arise instantaneously either by an alteration in the nuclear charge due to a radioactive disintegration or by a rapid loss of the core electron such as in photoionization and electron- and ion-induced ionizations.[56] The average excitation energy involved in the shakeup and shakeoff events can be approximated by 1.8 times the binding energy of the subshell from which the event occurs, and the threshold energy for a shakeoff event is near the binding energy.[56,57] For a given atom, the probability of the events largely increases with the principal quantum number of the shaking shell. In an atomic system, the shakeup of inner-shell electrons is relatively unimportant, but for the outermost shells the shakeup and shakeoff are nearly of equal importance. For an atom that is in a condensed medium or is part of a molecule, the event probabilities for the valence shells will be considerably altered though essentially unchanged for the inner shells.

In a metal, the binding energies of the orbital electrons are several eV less than those in the corresponding free atoms (or ions), since the former refer to the Fermi level and the latter to the vacuum level, and the outgoing electron in a shakeoff event need not escape from the metal but is shaked up to the Fermi level (shakeoff and shakeup merge into shakeup), accompanied by an extra-atomic relaxation of the atomic orbitals. As a consequence, the metallic effect leads to a notable decrease of the threshold required for these shakeup events. Therefore, the shakeup probability greatly rises, particularly for the outermost shells. This argument is reasonable. In previous studies of the satellite and diagram L x-ray spectra induced by electron impact on metallic zirconium and by x-ray photons incident on silver metal, the author[18] found that the M-electron shakeup probabilities due to a hole in the L shell are about 1.4 and 1.7 times as large as the calculations for the free atoms, respectively. We may expect that the shakeup probabilities of the more outer shells, Y (Y denotes the N, O, P, and Q shells), remarkably increase, and that the Y electrons are heavily stripped off by the shakeup, particularly for heavy elements (note that some of the valence electrons moved into the conduction band when the atomic system was condensed to the metallic state). For these atoms in a metal with atomic number Z, the Y electrons behave as if they appear in an atom with atomic number $Z+Z'$, and we can see from Fig. 5 that the f_{23} value will drop. Furthermore, the number of Y electrons that participate in the L_2-L_3Y Coster-Kronig process is obviously reduced, and so the f_{23} value will further decrease.

In summary, because there are many free electrons in the conduction band and the binding energies of the orbital electrons refer to the Fermi level in metals, the metallic effects reduce the electron binding energies, increase the total relaxation energy due to a core hole, and decrease the L_2-L_3Y Coster-Kronig yields of the heavy elements. In addition, the metallic effects lead to a decrease in the electron shakeoff thresholds, an increase in the shakeup (and shakeoff) probabilities of the outer electrons, and thus a further reduction of the L_2-L_3Y transition yields. For a given element the L-shell Coster-Kronig process in a chemical compound is more similar to that in the atomic system because there are few or no free electrons there.

The above philosophy can be also used to explain the decrease of the L_1-L_3 Coster-Kronig yields, f_{13}, of Ag, Sm, etc., measured by the synchrotron photoionization of the elemental metals[9,10] with respect to the theoretical calculations (many-body effects should be added). In fact, the surprisingly small value for the Sm L_1-L_3 Coster-Kronig transition, f_{13}(Sm)=0.18, reported by Stötzel *et al.*,[9] is well in line with the value of the Ag L_1-L_3Y Coster-Kronig yield f_{13Y}(Ag)=0.179, which was suggested in 1977 by Chen *et al.*[58] in order to interpret the Ag L x-ray satellite and diagram spectrum induced by x-ray photoionization of silver metal, and also with f_{13Y}(Ag)=0.177, which is obtained from the values of f_{13M}=0.37 (Ref. 17) and f_{13}=0.547 (Ref. 59) derived from the L x-ray measurements for proton impact on silver targets.

IV. CONCLUSIONS

The relative fluorescence yields of atomic L_1, L_2, and L_3 subshells of metallic uranium and thorium, ω_2/ω_3 and ω_1/ω_3, were derived from published L x-ray spectra produced by 50-keV electron impact on a uranium metal and thorium alloy and recorded with a curved mica crystal spectrometer. The present values of $\omega_2/\omega_3=1.39$ and $\omega_2=0.553$ for U and $\omega_2/\omega_3=1.38$ and $\omega_2=0.532$ for Th are all much large than the latest DHS calculations, semiempirical compilations, and measurements using the radionuclide sources to create initial inner vacancies, but are well in line with the experimental data obtained by means of the synchrotron photoionization and the electron- and proton-induced ionization of the elemental metals with $72 \leq Z \leq 83$. As a first test, using the present U L-subshell fluorescence yields and the ECPSSR ionization cross sections we calculated the relative L x-ray intensities I_β/I_α, I_γ/I_α, and $I_{\text{total}}/I_\alpha$ induced by few-MeV proton bombardment on metallic uranium, and it was found that the experimental L x-ray intensities are far more favorable to calculations using the present fluorescence yields than to those using the other yields.

To explain the deviations among ω_2 (and f_{23}) values of the heavy elements obtained from the theory and different measurements, the metallic state effects on the electron binding energies, the relaxation, the shakeoff and shakeup events, and the L-vacancy decay yields have been studied in this work. In consequence, we attribute deviations between the present yields and the others mainly to metallic effects. For a given system from free atoms to the metallic state, the orbital-electron binding energies of the atoms (or ions) decrease, the kinetic energies of the L_2-L_3 Coster-Kronig electrons and the shakeup probabilities of the outer-orbital electrons increase, the transition rate of the L_2-L_3 Coster-Kronig processes drop, and then the L_2-subshell fluorescence yields ascend because of the presence of the free electrons and the Fermi level in the metal. Measurements using radionuclides in some chemical compounds are more near the theoretical data for the corresponding free atoms. It follows that at least two sets of databases for the L-subshell vacancy transition yields should be established: one that is favorable to the atomic system, and another that is favorable to the metallic one. Hence more experimental data from different laboratories, where various elemental specimens and measuring techniques are employed, are expected.

ACKNOWLEDGMENT

The present research was supported by the National Natural Science Foundation of China.

*Permanent address: Shanghai Institute of Nuclear Research, Academia Sinica, P.O. Box 800-204, Shanghai 201800, China.

[1]M. H. Chen, B. Crasemann, and H. Mark, Phys. Rev. A **24**, 177 (1981).

[2]K. R. Karim, M. H. Chen, and B. Crasemann, Phys. Rev. A **29**, 2605 (1984); K. R. Karim and B. Crasemann, *ibid.* **31**, 709 (1985).

[3]M. H. Chen, B. Crasemann, N. Mårtensson, and B. Johansson, Phys. Rev. A **31**, 556 (1985).

[4]M. H. Chen, in *X-Ray and Inner-Shell Processes,* edited by T. A. Carlson, M. O. Krause, and S. T. Manson (American Institute of Physics, New York, 1990), p. 391.

[5]S. Fritzsche, B. Fricke, and W. D. Sepp, Phys. Rev. A **45**, 1465 (1992).

[6]M. Ohno, J. Phys. C **17**, 1437 (1984); J. M. Mariot and M. Ohno, Phys. Rev. B **34**, 2182 (1986).

[7]U. Werner and W. Jitschin, Phys. Rev. A **38**, 4009 (1988).

[8]W. Jitschin, G. Grosse, and P. Röhl, Phys. Rev. A **39**, 103 (1989).

[9]R. Stötzel, U. Werner, M. Sarkar, and W. Jitschin, Phys. Rev. A **45**, 2093 (1992); J. Phys. B **25**, 2295 (1992).

[10]S. L. Sorensen, R. Carr, S. J. Schaphorst, S. B. Whitfield, and B. Crasemann, Phys. Rev. A **39**, 6241 (1989); S. L. Sorensen, S. J. Schaphorst, S. B. Whitfield, and B. Crasemann, *ibid.* **44**, 350 (1991).

[11]J. L. Campbell, P. L. McGhee, R. R. Gringerich, R. W. Ollerhead, and J. A. Maxwell, Phys. Rev. A **30**, 161 (1984).

[12]P. L. McGhee and J. L. Campbell, J. Phys. B **21**, 2295 (1988); J. L. Campbell and P. L. McGhee, J. Phys. (Paris) Colloq. **38**, C9-597 (1987).

[13]A. L. Catz, Phys. Rev. A **36**, 3155 (1987); **40**, 4977 (1989); A. L. Catz and M. F. Meyers, *ibid.* **41**, 271 (1990).

[14]P. Putila-Mäntylä, M. Ohno, and G. Graeffe, J. Phys. B **17**, 1735 (1984).

[15]P. Amorim, L. Salgueiro, F. Parente, and J. G. Ferreira, J. Phys. B **21**, 3851 (1988).

[16]J. Auerhammer, H. Genz, and A. Richter, Z. Phys. D **7**, 301 (1988).

[17]J. Q. Xu and E. Rosato, Phys. Rev. A **37**, 1946 (1988); Nucl. Instrum. Methods B **33**, 297 (1988).

[18]J. Q. Xu, Z. Phys. D **13**, 25 (1989); J. Phys. B **23**, 1423 (1990).

[19]J. Q. Xu, Phys. Rev. A **43**, 4771 (1991).

[20]M. O. Krause, J. Phys. Chem. Ref. Data **8**, 307 (1979); M. O. Krause and J. H. Oliver, *ibid.* **8**, 329 (1979).

[21]P. Weightman, Rep. Prog. Phys. **45**, 753 (1982).

[22]S. Svensson, N. Mårtensson, E. Basilier, P. Å. Malmqvist, U. Gelius, and K. Siegbahn, J. Electron Spectrosc. **9**, 51 (1976); E. Antonides and G. A. Sawatzky, J. Phys. C **9**, L547 (1976).

[23]S. Datz, J. L. Duggan, L. C. Feldman, E. Laegsgaard, and J. U. Andersen, Phys. Rev. A **9**, 192 (1974); F. Abrath and T. J. Gray, *ibid.* **9**, 682 (1974); **10**, 1157 (1974); T. K. Li, D. L. Clark, and G. W. Greenless, *ibid.* **14**, 2016 (1976); Phys. Rev. Lett. **37**, 1209 (1976).

[24]D. D. Cohen and M. Harrigan, At. Data Nucl. Data Tables **34**, 393 (1986); Nucl. Instrum. Methods B **15**, 576 (1986).

[25]J. Q. Xu, Phys. Rev. A **44**, 373 (1991); J. Q. Xu and X. J. Xu, J. Phys. B **25**, 695 (1992); Phys. Rev. A **49**, 2191 (1994).

[26]M. Goldberg, Ann. Phys. (Paris) **7**, 329 (1962).

[27]J. G. Ferreira, M. O. Costa, M. I. Goncalves, and L. Salgueiro, J. Phys. (Paris) **26**, 5 (1965); L. Salgueiro, M. T. Ramos, M. L. Escrivào, M. C. Martins, and J. G. Ferreira, J. Phys. B **7**, 342 (1974).

[28]J. H. Scofield, Phys. Rev. A **18**, 963 (1978).

[29]S. Reusch, H. Genz, W. Löw, and A. Richter, Z. Phys. D **3**, 379 (1986).

[30]A. Kodre, M. Hribar, B. Ajlec, and J. Pahor, Z. Phys. A **303**,

23 (1981).
[31]M. Tan, R. A. Braga, and R. W. Fink, Phys. Scr. **25**, 536 (1982).
[32]P. V. Rao, Bull. Am. Phys. Soc. **33**, 943 (1988).
[33]A. Laakkonen and G. Graeffe, J. Phys. (Paris) Colloq. **48**, C9-605 (1987); M. Ohno, A. Laakkonen, A. Vuoristo, and G. Graeffe, Phys. Scr. **34**, 146 (1986).
[34]J. C. Fuggle and S. F. Alvarado, Phys. Rev. A **22**, 1615 (1980).
[35]J. H. Scofield, Phys. Rev. A **10**, 1507 (1974); **12**, 345(E) (1975).
[36]J. L. Campbell and J. X. Wang, At. Data Nucl. Data Tables **43**, 281 (1989).
[37]J. C. McGeorge, D. W. Nix, R. W. Fink, and J. H. Landrum, Z. Phys. **255**, 335 (1972).
[38]J. C. McGeorge and R. W. Fink, Z. Phys. **248**, 208 (1971).
[39]K. Sieber, A. M. M. Mohammedein, G. Musiol, I. Reiche, and G. Zschornack, Nucl. Instrum. Methods B **68**, 292 (1992); T. Papp, J. L. Campbell, and S. Raman, J. Phys. B **26**, 4007 (1993).
[40]J. H. Scofield, At. Data Nucl. Data Tables **14**, 121 (1974).
[41]D. D. Cohen and M. Harrigan, At. Data Nucl. Data Tables **33**, 255 (1985).
[42]W. Brandt and G. Lapicki, Phys. Rev. A **23**, 1717 (1981).
[43]B. B. Dhal, T. Nandi, and H. C. Padhi, Phys. Rev. A **49**, 329 (1994).
[44]R. S. Sokhi and D. Crumpton, At. Data Nucl. Data Tables **30**, 49 (1984); I. Orlic, C. H. Sow, and S. M. Tang, *ibid.* **56**, 159 (1994).
[45]M. H.Chen and B. Crasemann, At. Data Nucl. Data Tables **41**, 257 (1989).
[46]J. L. Campbell, Nucl. Instrum. Methods B **31**, 518 (1988).
[47]P. B. Semmes, R. A. Braga, J. C. Griffin, and R. W. Fink, Phys. Rev. C **35**, 749 (1987).
[48]F. P. Larkins, J. Phys. B **9**, 47 (1976); J. M. Crotty and F. P. Larkins, *ibid.* **9**, 881 (1976).
[49]L. Ley, S. P. Kowalczyk, F. R. McFeely, R. A. Pollak, and D. A. Shirley, Phys. Rev. B **8**, 2392 (1973); S. P. Kowalczyk, L. Ley, F. R. McFeely, R. A. Pollak, and D. A. Shirley, *ibid.* **9**, 381 (1974).
[50]E. Antonides, E. C. Janse, and G. A. Sawatzky, Phys. Rev. B **15**, 1669 (1977); **15**, 4596 (1977).
[51]F. P. Larkins, J. Phys. C **10**, 2453 (1977); **10**, 2461 (1977).
[52]F. P. Larkins, At. Data Nucl. Data Tables **20**, 311 (1977).
[53]P. Weightman, P. T. Andrews, and L. A. Hisscott, J. Phys. F **5**, L220 (1975).
[54]J. Tulkki and A. Mäntykenttä, Phys. Rev. A **47**, 2995 (1993).
[55]H. B . Michaelson, in *CRC Handbook of Chemistry and Physics,* edited by D. R. Lide (CRC Press, Boston, 1992), pp. 12–97.
[56]T. A. Carlson, C. W. Nestor, Jr., T. C. Tucker, and F. B. Malik, Phys. Rev. **169**, 27 (1968); T. A. Carlson and C. W. Nestor, Jr., Phys. Rev. A **8**, 2887 (1973).
[57]T. A. Carlson, Radiat. Res. **64**, 53 (1975).
[58]M. H. Chen, B. Crasemann, M. Aoyagi, and H. Mark, Phys. Rev. A **15**, 2312 (1977).
[59]E. Rosato, Nucl. Instrum. Methods B **15**, 591 (1986).